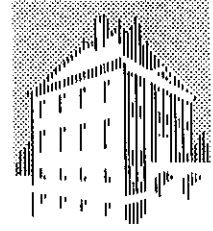


DECEMBER 1993

FOM-INSTITUUT  
VOOR  
PLASMAFYSICA  
RIJNHUIZEN



ASSOCIATIE  
EURATOM-FOM

## 3-D SIMULATIONS OF THE FEM OSCILLATOR FOR FUSION AT 130-250 GHz

A.V. TULUPOV, M.J. VAN DER WIEL, W.H. URBANUS AND M. CAPLAN

RIJNHUIZEN REPORT 93-216

This work was performed as part of the research programme of the association agreement of Euratom and the 'Stichting voor Fundamenteel Onderzoek der Materie' (FOM) with financial support from the 'Nederlandse Organisatie voor Wetenschappelijk Onderzoek' (NWO) and Euratom.

POSTBUS 1207  
3430 BE NIEUWEGEIN  
NEDERLAND  
EDISONBAAN 14  
3439 MN NIEUWEGEIN  
TEL. 03402 - 31224  
TELEFAX 03402 - 31204

## C O N T E N T S

	page
Abstract	1
1. Introduction	2
2. Linear gain and output power	3
3. FEM operation at 130 GHz	5
4. The influence of the undulator parameters on the FEM operation	8
5. Influence of the emittance	10
6. Conclusions	14
References	14

# 3-D SIMULATIONS OF THE FEM OSCILLATOR FOR FUSION AT 130-250 GHz

A.V. Tulupov, M.J. van der Wiel, W.H. Urbanus

*FOM-Instituut voor Plasmafysica 'Rijnhuizen', Association EURATOM-FOM,*

*P.O. Box 1207, 3430 BE Nieuwegein, The Netherlands*

M. Caplan

*Lawrence Livermore National Laboratory, P.O. Box 808 L440,*

*Livermore, CA 94550, USA*

## **Abstract**

The performance of a 1 MW, long-pulse, 130-250 GHz free-electron maser for fusion applications, which is being designed at the FOM-Institute for Plasma Physics, has been simulated. The CRMFEL code, a fully 3-D, AC and DC space-charge included, non-wiggle averaged, particle-pusher code has been used. In comparison with previous designs a shorter construction of a step-tapered undulator is considered. It provides suppression of double frequency amplification during the linear stage (start-up) and a perfect matching of the power growth during the nonlinear stage (saturated regime). The dependencies of the linear gain and the output power on the operating frequency, the reflection coefficient of the mm-wave cavity, the gap length between the two undulator sections and the electron beam focusing efficiency are examined. Particular attention has been devoted to the influence of space charge on the operation of the FEM oscillator. Longitudinal space charge reduces the linear gain but increases the level of power which can be reached inside the resonator. It is shown that for the chosen undulator length there is an optimum value of the electron beam current density which provides sufficiently high linear gain and output power.

## 1. Introduction

Localized plasma heating, magnetic island stabilization and current drive experiments in tokamak installations are areas of intensive magnetic fusion research that would be promoted greatly by the availability of a high average power, high frequency, tunable microwave source. The aim of the design of the FEM oscillator being developed at Rijnhuizen is to provide an attractive source of mm-wave radiation for fusion applications. The FOM-FEM should meet the following parameters: a frequency of 130-250 GHz, an output power of 1 MW, a system efficiency exceeding 35%.

To satisfy these parameters a MeV DC accelerator with a beam current of 12 A and an undulator consisting of two sections with a step taper will be used [1,2]. In the previous design of the undulator, 24 full periods with a peak field of 2 kG in the first section and 17 full periods with a peak field of 1.7 kG in the second section (the undulator period equals to 4 cm) were considered. Although this construction permitted to reach the required output power there were several disadvantages.

Firstly, the linear gain curve (the detuning curve) had two peaks at different frequencies [2]; one was due to the radiation in the first section and the other one originated from the second undulator section. Moreover, the gain at the second frequency was even larger than the gain at the required operating frequency. The resonance frequencies of the two undulator sections were too close. A small modulation of the electron energy in the first section led to the prebunching of the beam and, hence, to an increase of the gain in the second section. The possibility of double frequency generation was real. At the nonlinear amplification stage the presence of two frequencies in the radiation spectrum can lead to frequency multiplication. So it was reasonable to shorten the length of the second section and to decrease the amplitude of the magnetic field (first simulation results were presented in Ref. [2]). This change also suppresses spontaneous emission from the second undulator section.

Secondly, in the nonlinear regime the dependency of the power on the distance along the undulator had a dip at the beginning of the second section [1,2]. Hence, in the second section electrons first had to be rebunched slightly before further amplification of the e.m. wave. It means that at the end of the first section the electron beam did not have an optimum bunching parameter value or, in other words, the first undulator section was too long.

Thirdly, the dependency of the power on the length of the system demonstrated over-saturation of the signal near the end of the first section [1,2]. This is dangerous because of a possible development of sideband instability followed by widening of the spectrum and oscillations of the efficiency, particularly due to the long operation period of the FEM (100 ms). This fact also required a shorter first undulator section.

Having taken into account these three disadvantages we have changed the undulator design. In this paper simulations of the new design are presented. Comparing with the former results [2] simulations have been extended to the low frequency region near 130 GHz.

## 2. Linear gain and output power

An undulator of two sections with 20 full periods and a peak magnetic field of 2 kG in the first section and 14 full periods and a peak magnetic field of 1.6 kG in the second section has been chosen. Between the two sections is a small gap without magnetic field. One period (4 cm) cells are used on both sides of the sections for matching of the electron beam (see insertion in Fig. 1). The mm wave propagates in a rectangular corrugated waveguide with a cross section of  $15 \times 20 \text{ mm}^2$ . In this type of waveguide a hybrid transverse mode,  $\text{HE}_{11}$ , is formed, which is strongly peaked at the centre.

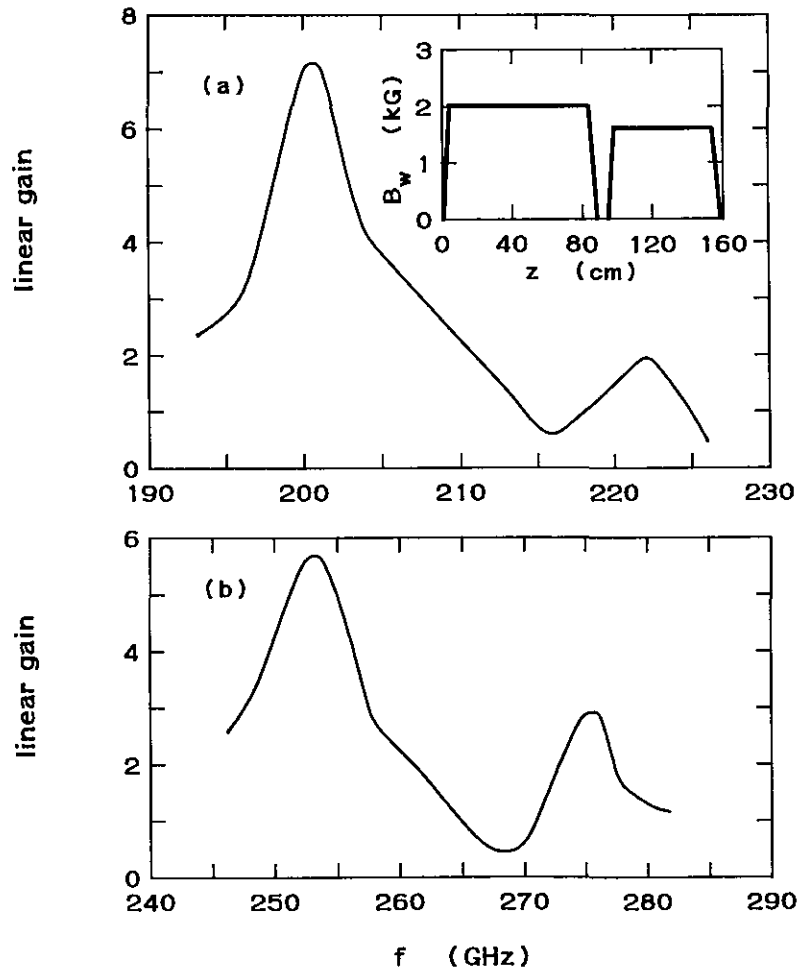


Fig. 1. Linear gain as a function of the frequency,  $f$ , of the input signal: a. electron energy  $E = 1.75 \text{ MeV}$ , b.  $E = 2.0 \text{ MeV}$ ,  $\epsilon_N = 50 \pi \text{ mm mrad}$ ,  $I = 12 \text{ A}$ .

The fully 3-D CRMFEL code [3] has been used. The main features of this code are: non-wiggle averaged electron trajectories, initial particles distribution in a uniform 4-volume corresponding to beam emittance, e.m. fields are expanded as a set of arbitrary waveguide modes, AC space charge is included up to the 5th harmonic of a ponderomotive wave frequency, DC space charge and arbitrary transverse focusing of the electron beam are included. This code runs only one frequency. First the detuning curves are calculated and then all nonlinear simulations are performed with the frequency corresponding to the maximum linear gain.

In Fig. 1 the linear gain curves are presented for beam energies of 1.75 and 2.00 MeV, where the main peaks correspond to frequencies of 201 and 253 GHz, respectively. Both curves have a double peak structure, but the height of the second peak is essentially lower than of the first one. In fact the height of the second peak defines partly the required value of the reflection coefficient of the resonator, because the condition  $gR > 1$  should be fulfilled for signal excitation, where  $g$  is the linear gain and  $R$  is the reflection coefficient,  $R = P_{\text{ref}}/P_{\text{tot}}$ , where  $P_{\text{tot}}$  is the total power coming out of the undulator and  $P_{\text{ref}}$  is the amount of power reflected back to the input of the waveguide system. In the FEM construction there is a possibility to tune the amount of power coming out from the FEM and change the reflection coefficient [1]. For  $R = 29\%$ , which is the optimum value for a given emittance of the electron beam and the undulator length in the nonlinear regime (see below), it is evident that higher frequency peaks for both electron energies cannot be excited.

The value of the emittance is equal to  $50 \pi$  mm mrad which corresponds to a beam radius of about 1 mm. The detailed study of the influence of the emittance on the gain and the saturated power is presented in Sec. 4. Here we only notice that  $\epsilon_N = 50 \pi$  mm mrad provides simultaneously sufficiently high linear gain, required output power and frequency (at a lower emittance the frequency with the maximum growth rate is shifted towards lower values). Gain curves have been calculated for a beam current  $I = 12$  A. Peak gain values are lower than in the previous design [2], but sufficiently high to overcome the generation threshold at  $R = 29\%$  and to reach saturation during  $1 \mu\text{s}$ .

Figure 2 shows the net mm-wave power as a function of the longitudinal coordinate at frequencies of 201 and 253 GHz (beam energy 1.75 and 2.00 MeV, respectively) for the stationary regime. The input power is different for different energies, it is defined by the relation  $P_{\text{in}} = RP_{\text{tot}}$ , where  $P_{\text{tot}} = P_{\text{in}} + P_{\text{net}}$ . Both curves demonstrate good matching between the two sections of the undulator. From one side, the mm wave reaches the saturation level, that is the maximum efficiency is provided. From the other side, there is no over-saturation and remarkable rebunching at the entrance of the second section. These conditions are optimal for a narrow spectrum generation. All curves were obtained at  $\epsilon_N = 50 \pi$  mm mrad.

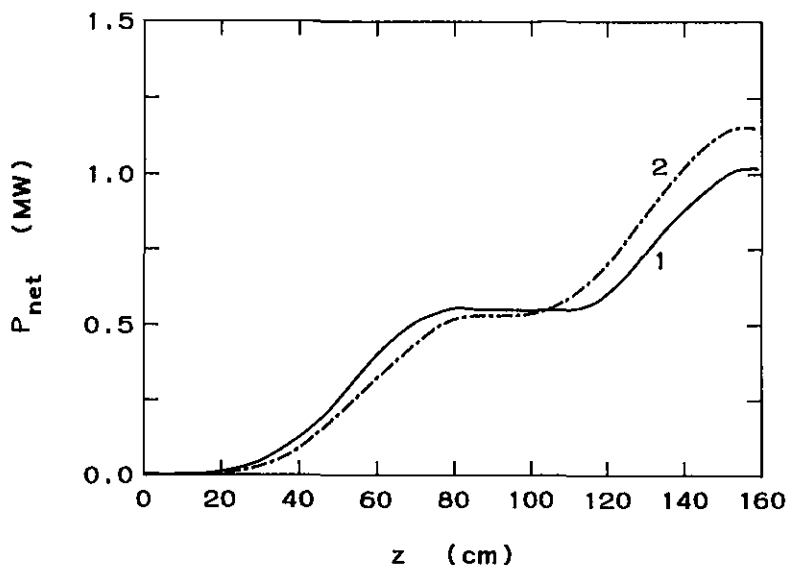


Fig. 2. Net mm-wave power as a function of the position in the undulator,  $z$ , in the nonlinear regime:  
 1.  $E = 1.75$  MeV,  $f = 201$  GHz; 2.  $E = 2.0$  MeV,  $f = 253$  GHz,  $R = 0.29$ ,  $\epsilon_N = 50 \pi$  mm mrad,  
 $I = 12$  A.

The dependencies of the net output power on the reflection coefficient are shown in Fig. 3. One can see that the optimum  $R$  is different for different beam energies and maximum power is shifted to a higher reflection coefficient with increasing electron energy. This fact is connected with the reduction of the nonlinear gain for increased energy. Because of this fact a more powerful input signal or higher reflection coefficient is necessary to get saturation at a fixed length of the undulator. Nevertheless, there is a region of the reflection coefficient which is convenient for both electron energies; it lies near  $R = 29\text{-}35\%$ . As has been mentioned above, to suppress possible double frequency generation the reflection coefficient value should be as low as possible. For  $E = 1.75$  MeV the reflection coefficient dependency (curve 1 in Fig. 3) is sufficiently flat and the amplitude of the high frequency peak (Fig. 1a) is low, hence,  $R$  can be varied in a wide range ( $R \sim 25\text{-}37\%$ ). In the case of  $E = 2.0$  MeV, however, the range of possible variation of  $R$  is essentially more restricted. One can see (Fig. 1b) that the difference in height of the two linear gain peaks is small:  $g = 5.62$  at  $f = 253$  GHz and  $g = 2.86$  at  $f = 276$  GHz. It means that at a higher value of  $R$  (near 35%) the second frequency can be excited, but at a lower value of  $R$  (less than 28%) the start-up time of the oscillator increases and the output power drops sharply. So,  $R = 29\%$  is the optimum value.

### 3. FEM operation at 130 GHz

The possibility of low frequency generation near 130 GHz has been considered too. Our simulations show that the situation is different in comparison to the tuning of the FEM from 200 to 250 GHz. In this case to obtain satisfactory results it is not enough to simply diminish the electron beam energy. Some other parameters should also be changed. In order to get high

output power the current should be fixed at the highest value,  $I = 12$  A. The most simple way is changing the reflection coefficient.

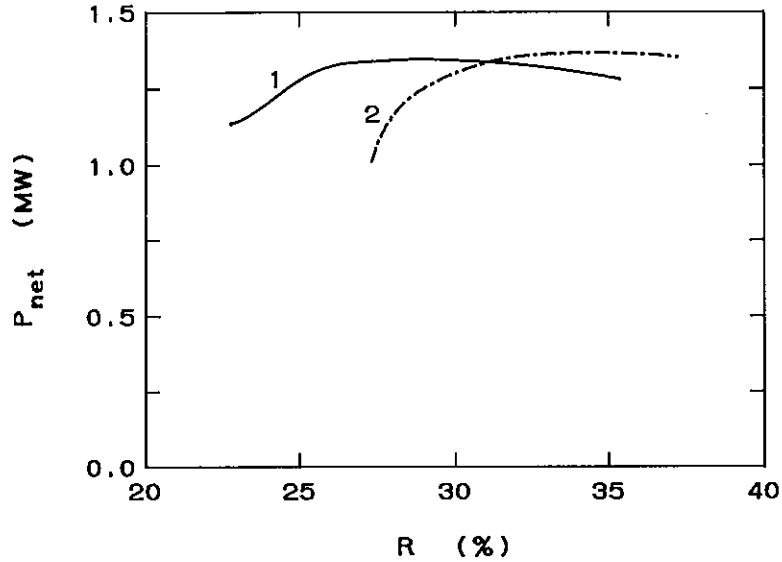


Fig. 3. Net output power as a function of the reflection coefficient, R: 1. 201 GHz, 2. 253 GHz.

Figure 4a illustrates the linear gain dependency, which is double-peaked. The peaks lie very close. Their height is comparable, hence, to avoid double frequency generation or even broad band generation, one should be very careful with the choice of the reflection coefficient. Curve 1 on Fig. 5 shows the dependency of the net output power on the reflection coefficient. One can see that the power is at maximum near  $R = 15\%$ . The corresponding extraction efficiency in this case is  $\eta = 9.2\%$ , which is very high. The condition  $gR = 1$ , however, requires that the R-value does not exceed  $11\%$  in order to suppress the second peak on the linear gain curve. This value of the reflection coefficient corresponds to the descent on the net power curve (Fig. 5) and decreasing of the efficiency to  $\eta = 7\%$ . Even in this case the net output power exceeds 1 MW (see curve 1 in Fig. 6), and it grows successfully along the length of the undulator.

To increase the efficiency it is necessary to change the amplitude of the magnetic field in the second undulator section. If the peak field value is diminished from 1.6 to 1.5 kG the linear gain curve is changed significantly. The second peak is shifted to the higher frequency region and becomes very low (Fig. 4b). At these conditions there are no restrictions imposed on the reflection coefficient. The dependency of  $P_{\text{net}}$  is more flat (curve 2 in Fig. 5) and the decline of power corresponds to the lower values of R. In this case the FEM can operate at the maximum efficiency  $\eta > 8\%$  and the net power is near 1.15 MW (curve 2 in Fig. 6 corresponds  $\eta = 8.3\%$ ). Of course, changing the amplitude of the magnetic field is a major procedure.



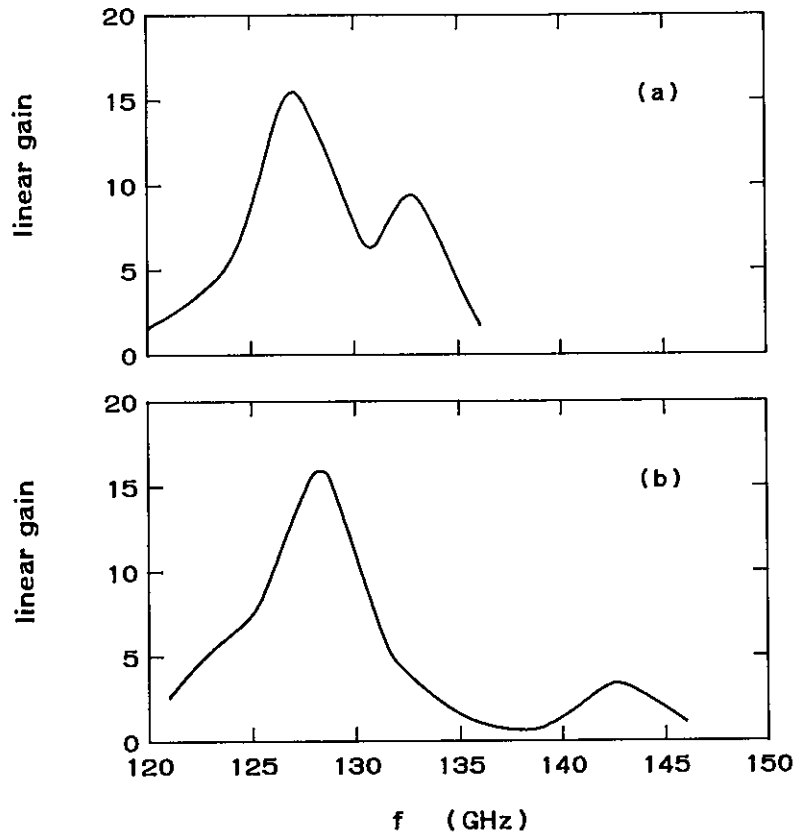


Fig. 4. Linear gain curves as a function of the input signal frequency,  $f$ , for  $E = 1.35$  MeV:  
 a. with the peak magnetic field in the second section  $B_{w2} = 1.6$  kG,  
 b. with  $B_{w2} = 1.5$  kG,  $\epsilon_N = 50 \pi$  mm mrad,  $I = 12$  A.

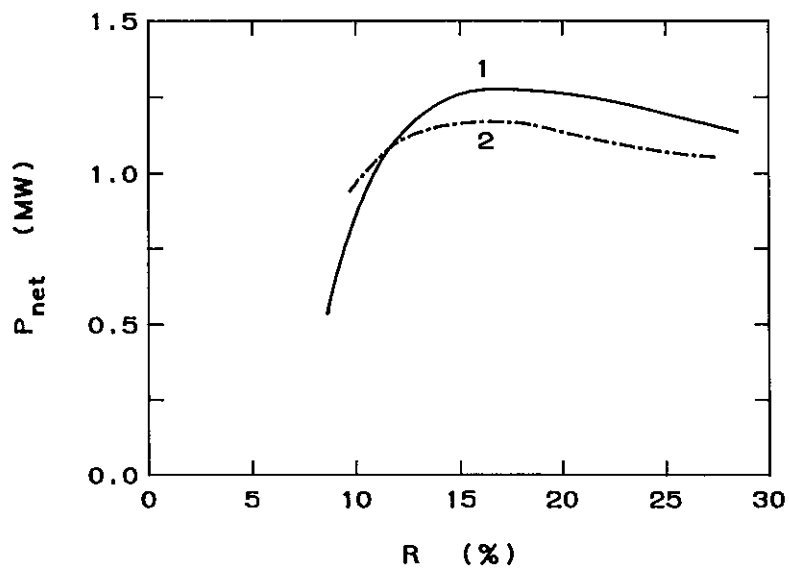


Fig. 5. Net output power as a function of the reflection coefficient,  $R$ :  $E = 1.35$  MeV,  $f = 128$  GHz:  
 1.  $B_{w2} = 1.6$  kG; 2.  $B_{w2} = 1.5$  kG.

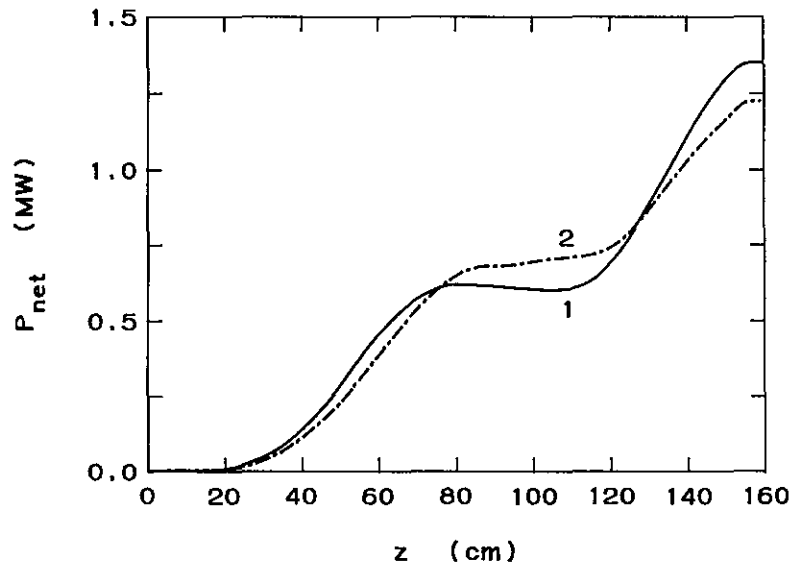


Fig. 6. Net mm-wave power as a function of the position in the undulator length,  $z$ :  $E = 1.35$  MeV,  $f = 128$  GHz: **curve 1.** reflection coefficient  $R = 11\%$ ,  $B_{w2} = 1.6$  kG; **curve 2.**  $R = 15\%$ ,  $B_{w2} = 1.5$  kG.

#### 4. The influence of the undulator parameters on the FEM operation

In the conventional FEL scheme all undulator parameters are fixed. In our design there are possibilities to change some parameters after the undulator will have been built, namely the length of the gap between the two undulator sections and the transverse focusing strength.

In the gap between the two undulator sections the magnetic field is equal to zero. Therefore, during the motion of electrons along this drift space bunching is being modified. The degree of this modification depends on the drift length, which results in a change of the linear gain and saturated power. In Fig. 7 results of simulations of the FEM performance for different gap lengths are presented ( $E = 1.75$  MeV). The curves for the linear gain and the output power oscillate periodically. That is connected with a variation of the phase of the electrons along the gap length. There are regions where the output power is lower than the required value of 1 MW, but there are also regions where it is essentially higher. The peaks of both curves are shifted. Hence, from the point of bunching, the optimum drift conditions for the linear gain and saturated power do not coincide. Nevertheless, near  $L_g = 60$  mm, 110 mm etc., the saturated power is at maximum and the linear gain is near the maximum value. Since the shorter gap is always more preferable to provide better transportation of the electron beam, the value of 60 mm has been chosen for all simulations presented above.

These oscillatory dependencies give a good experimental possibility to vary the linear gain or output power independently. Changing the gap length one can go to lower values of the gain without decreasing the saturated power. It might be a possibility to suppress parasitic longitudinal mode excitation if it appears in experiments.

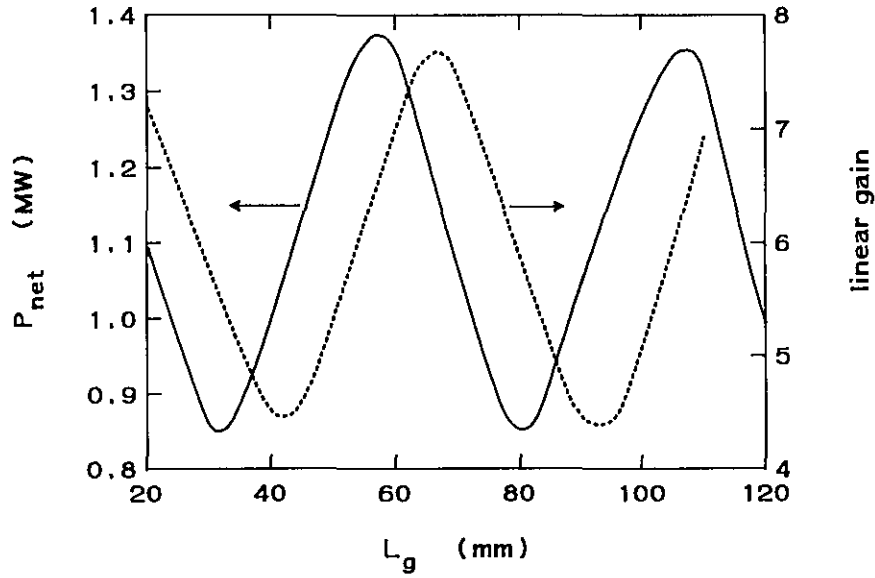


Fig. 7. The linear gain and the net saturated power as a function of the gap length between the two undulator sections,  $E = 1.75$  MeV.

Another possibility of adjusting the oscillator is linked with a specific transverse beam focusing system of the undulator. Usually transverse beam focusing is provided by using magnets with parabolic poles [4]. In the case of the FOM-FEM another focusing system will be applied. Apart from the main magnet arrays two periodic side magnets for field shaping will be present. Variation of the field shape gives a focusing field similar to the field obtained by parabolic poles. Therefore the fine tuning of the magnetic field focusing can be implemented. This tuning permits changing the focusing properties of the undulator, that is changing the degree of overlapping of the electron beam and the mm wave inside the waveguide.

Our simulations showed that at the electron energy  $E = 2.0$  MeV a non-resonant parasitic  $HE_{13}$  mode can be excited slightly (there is no such excitation for lower electron energies). We studied how this excitation depends on the beam distribution in the transverse plane. Results are illustrated in Fig. 8, where the dependencies of the total linear gain and the net  $HE_{11}$  gain on the focusing ratio  $k_{\beta y}/k_{\beta x}$  are presented ( $yOz$  is the plane of the undulator motion), where  $k_{\beta y}$  and  $k_{\beta x}$  are the betatron wavenumbers in the transverse direction. One can see that the linear gain is changed significantly with the focusing ratio. The case of equal focusing,  $k_{\beta y} = k_{\beta x}$ , is the most convenient, since it corresponds to the lowest difference between the total gain and the net  $HE_{11}$  gain.

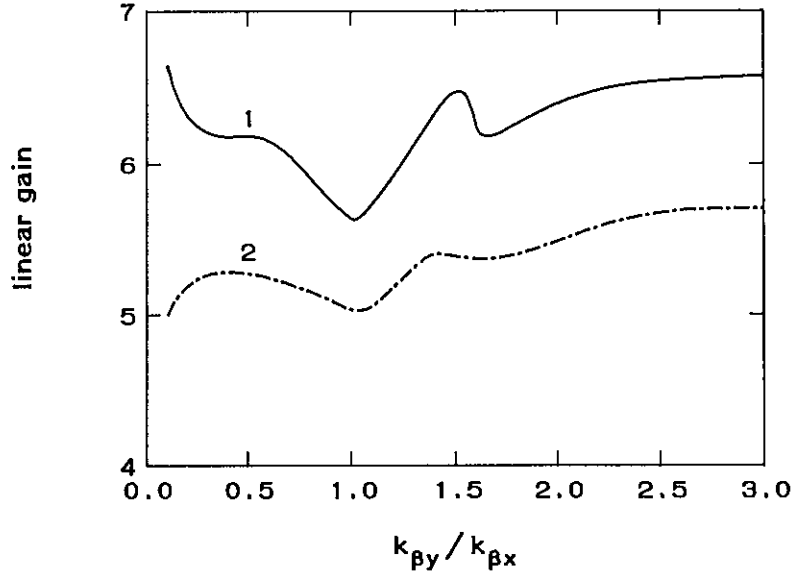


Fig. 8. The total linear gain (curve 1) and the net HE<sub>11</sub> gain (curve 2) as a function of the focusing ratio  $k_{\beta y}/k_{\beta x}$ :  $f = 253$  GHz and  $E = 2.0$  MeV.

## 5. Influence of the emittance

Though the dependency of FEL characteristics on the beam current density (beam emittance defines the radius of the beam and therefore the beam current density or plasma density of the beam) has been investigated from the beginning of FEL physics, there is no full clarity in this question yet. There are at least two parameters in the limits of idealized one-dimensional treatment (see review paper [5]) which define the importance of space-charge effects. The first parameter is obtained from the comparison of the linear gains in the high gain Compton and the Raman regime. The boundary value of the transverse electron velocity,  $\beta_{wb}$ , between the two regimes is given by

$$\beta_{wb} = \frac{3\sqrt{3}}{2} \left( \frac{\omega_b}{ck_w \gamma^{1/2} \gamma_z^3} \right)^{1/2}, \quad (1)$$

where  $\omega_b$  is the electron beam plasma frequency and  $k_w = 2\pi/\lambda_w$ ,  $\lambda_w$  is the undulator period. The second parameter is connected with the length of the undulator, which should be long enough for several plasma oscillations.

A more complicated study of space-charge effects was implemented by Scharlemann et al. in Refs [6] and [7]. They demonstrated numerically that the gain was reduced due to the action of the longitudinal space-charge electric fields produced by the electron bunches on the bunching efficiency. The simulations showed also that the output power of the FEL amplifier became smaller for higher value of the beam brightness [7] (smaller values of emittance). However, all

simulations were done for a fixed undulator length and at the particular value of the emittance the wave did not reach saturation. Hence, it was unclear whether the saturated power level for the smaller emittance was higher or lower than for the larger one.

Recently, Freund found the importance of 3-D effects and the wiggly-averaged orbit approximation, which can alter the relative significance of the ponderomotive and space-charge potentials [8] (the results of Scharlemann et al. were based on a motion-averaged code).

Our simulations have shown (Fig. 9 and Ref. [2]) an increase of the linear gain with increasing emittance and a decrease of the net output power with decreasing emittance.

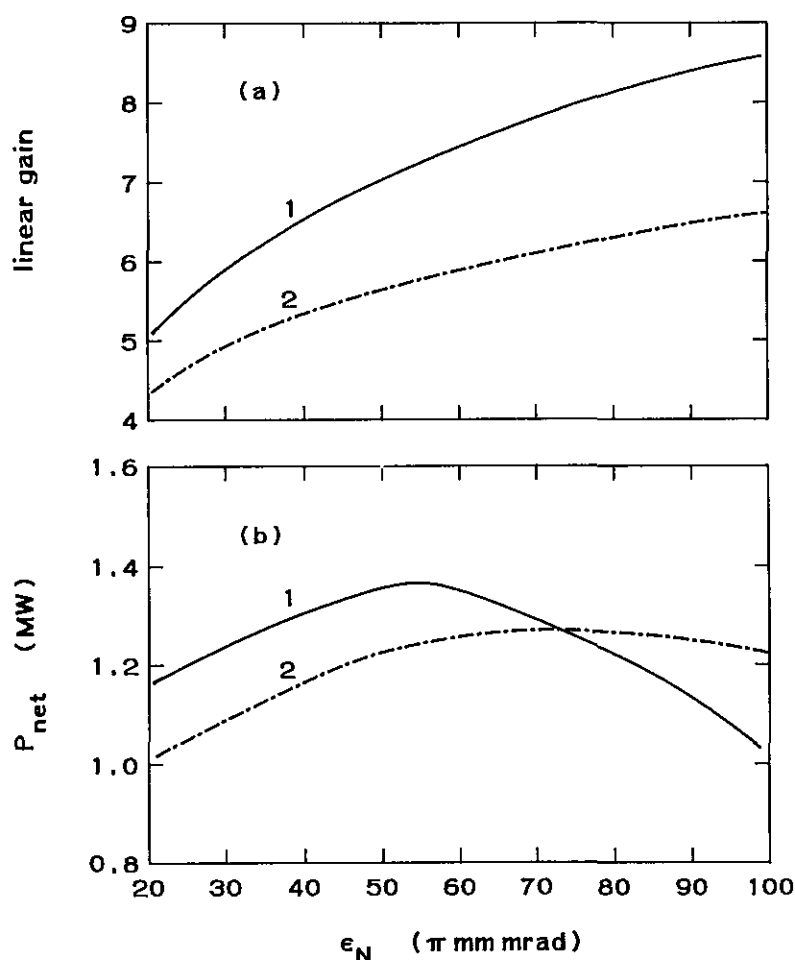


Fig. 9. The linear gain (a) and the net output power (b) as a function of the beam emittance,  $\epsilon_N$ :  
**curve 1.**  $E = 1.75$  MeV,  $f = 201$  GHz; **curve 2.**  $E = 2.0$  MeV,  $f = 253$  GHz.

Therefore, there are several questions which arise after considering the accumulated results about space-charge influence on the FEL operation:

- if the longitudinal space-charge forces reduce the linear gain should there be a peak on the gain curve at some beam emittance?

- if this peak value of the gain occurs, is it connected with some parameter from the 1-D analytical theory?
- if the frequency shift due to plasma oscillations is taken into account, will the saturated power be less for a lower emittance?

The CRMFEL code [3] includes the space-charge potential like it was done in the FRED code [6], but without the wiggler-averaged approximation. This code also permits comparing results with and without influence of the longitudinal space charge.

To clarify the situation we considered at first the linear gain as a function of emittance only for an undulator of one section with a period of 4 cm and a length of 80 cm (just the same like the first section in the FEM design, in fact only the first section defines the gain in the linear regime). Figure 10 represents linear gain curves as a function of the electron beam emittance for an electron beam energy of 1.75 MeV. Curve 1 is calculated with AC space charge included, curve 2 without space-charge influence. Both curves correspond to frequencies with the maximum growth rate. This frequency is changed in the range of 196 - 203 GHz and this variation is due to both space-charge and 3-D effects. The latter originates from the variation of the undulator magnetic field in the transverse direction.

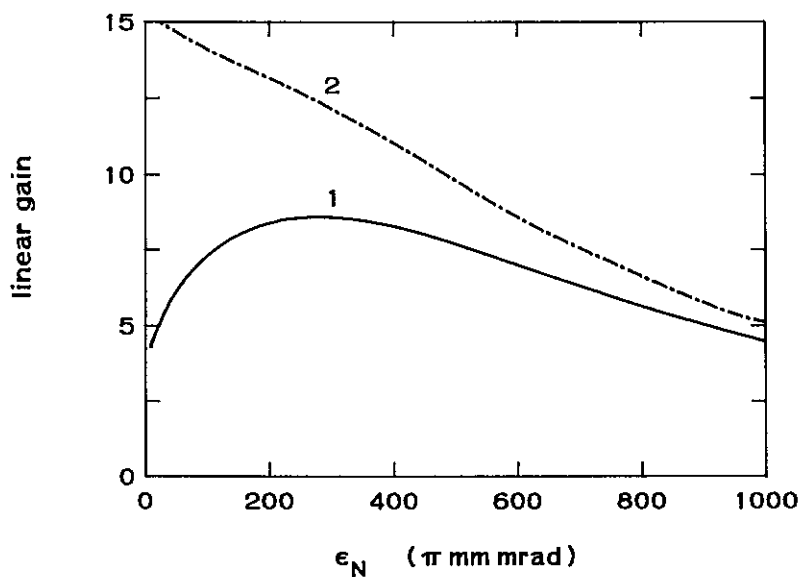


Fig. 10. The linear gain vs emittance,  $\epsilon_N$ , for a one-section undulator construction:  
 1. with space-charge effects; 2. without space-charge effects;  $E = 1.75$  MeV,  
 $I = 12$  A,  $L_w = 80$  cm.

Both curves behave in different ways. One can see that in the low emittance region the bunching efficiency is significantly suppressed as a result of the space-charge repulsion and there is an optimum emittance for the maximum linear gain. Only at a very high emittance, space-charge influence on the gain can be neglected. It is interesting that there is no correlation between the behaviour of curve 1 and the parameters obtained in the analytical 1-D theory.

None of them have a correspondence with the peak of the curve or with its falling down. The only value which can be predicted analytically with a sufficiently good accuracy is the emittance value at which space-charge acting on the gain can be neglected. As shown in Ref. [9], when  $k_b^2 L_w^2 \ll 1$ , where  $L_w$  is the length of the undulator, and  $k_b = \omega_b / \sqrt{24\gamma} \gamma_2 c$ , the space-charge forces are negligible. For our design the electron beam radius should satisfy the condition

$$r_b \gg \frac{L_w}{\gamma} \left( \frac{I}{6\gamma I_A} \left( 1 + \frac{a_w^2}{2} \right) \right)^{1/2} = 1.05 \text{ mm} , \quad (2)$$

where  $I_A$  is the Alfvén current and  $a_w$  is the undulator parameter. When  $\epsilon_N = 1000 \pi \text{ mm mrad}$ ,  $r_b = 4.1 \text{ mm}$ , and at this region gain curves with and without the longitudinal space-charge force have practically the same value.

As mentioned above, Fig. 9b shows results for a single, fixed frequency. To obtain the real saturated power level which can be reached at a particular emittance value, nonlinear simulations should be done at the frequency of the maximum growth rate as a function of the emittance. These simulation results are presented in Fig. 11 for the intra-cavity saturated power (curve 1) and the output power (curve 2). The real FEM design with two undulator sections has been considered in this case, because both undulators give practically the same contribution to the amplification on the nonlinear stage (see Figs 2, 8). Figure 11 shows that the saturated power level (inside the cavity) moves towards higher values with decreasing emittance. It means that though the space-charge repulsion reduces the nonlinear gain as well as the linear gain, the amplitude value of the mm wave at which electrons stop to amplify becomes larger.

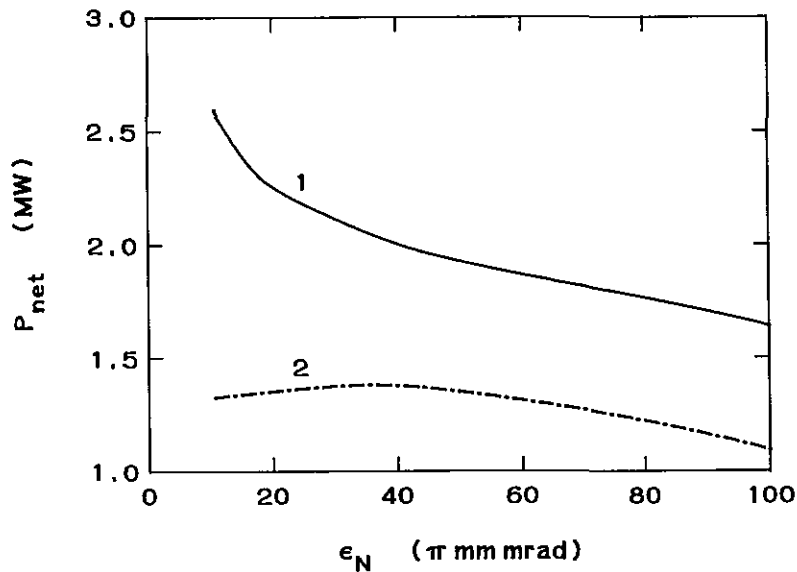


Fig. 11. Saturated power for the FEM design as a function of emittance,  $\epsilon_N$ :  
1. intracavity power, 2. output power:  $E = 1.75 \text{ MeV}$ ,  $I = 12 \text{ A}$ .

Therefore, the same degree of bunching of the electron beam for different emittances corresponds to different power levels. To reach this saturated power level for the fixed undulator length a stronger input signal is necessary. It requires a higher value of the reflection coefficient.

At some emittance the increase of the intra-cavity power cannot compensate the decrease of the output power due to the increase of the reflection coefficient. As a result the net output power becomes lower in the lower emittance region (curve 2, Fig. 11), but the slope of the curve is much lower than in Fig. 9b. The same result can be obtained for a FEM amplifier with a fixed undulator length: at some value of electron beam density the output power should become lower than for the smaller density, it simply means that the signal cannot reach the saturation due to nonlinear gain reduction.

## 6. Conclusions

1. The present design of the FEM provides sufficient linear gain and an output power more than 1 MW in the frequency range from 130 to 250 GHz.
2. The resonant frequency corresponding to the second undulator section is suppressed.
3. A shorter undulator construction demonstrates good matching of the undulator sections.
4. A change in the operation frequency from 200 to 250 GHz can be reached by increasing the electron energy without a variation of any other parameter.
5. Generation at 130 GHz requires at least two modifications: decreasing the energy of electron and the reflection coefficient. The amplitude of the magnetic field in the second undulator section should also be changed to reach optimal operation. However, without changing the magnetic field in the second undulator section, the output power still exceeds 1 MW.
6. A variation of the gap length between two undulator sections permits tuning of the linear gain and output power.
7. Equal focusing of the beam in the transverse direction provides the best conditions for suppression of parasitic transverse modes.
8. An increase of the beam density does not always designate an increase of the gain or (and) efficiency, and for each particular design with a fixed length there are optimum values of emittance and reflection coefficient to operate at the saturated level.

## References

- [1] W.H. Urbanus et al., Nucl. Instrum. and Methods Phys. Res., **A331** (1993) 235.
- [2] M. Caplan et al., Nucl. Instrum. and Methods Phys. Res., **A331** (1993) 243.
- [3] M. Caplan, Preprint UCRL-JC-107204, LLNL, 1991.
- [4] E.T. Scharlemann, J. Appl. Phys., **58** (1985) 2154.
- [5] C.W. Roberson and P. Sprangle, Phys. Fluids, **B1** (1989) 3.
- [6] E.T. Scharlemann, W.M. Fawley, B.R. Anderson and T.J. Orzechowski, Nucl. Instrum. Methods, **A250** (1986) 150.
- [7] R.A. Jong and E.T. Scharlemann, Nucl. Instrum. Methods, **A259** (1987) 254.
- [8] H.P. Freund, Nucl. Instrum. and Methods Phys. Res., **A331** (1993) 496.
- [9] C.M. Tang, P. Sprangle, J. Appl. Phys., **53** (1982) 831.